openheart

Aortic geometry and long-term outcome in patients with a repaired coarctation

Savine C S Minderhoud,[1,2] Rick van Montfoort,[1] Timion A Meijs,[3] Suze-Anne Korteland,[1] Jan L Bruse,[4] Isabella Kardys,[1] Jolanda J Wentzel,[1] Michiel Voskuil,[3] Alexander Hirsch ,[1,2] Jolien W Roos-Hesselink ,[1] Annemien E van den Bosch [1]

► Additional supplemental material is published online only. To view, please visit the journal online (https://doi.org/10.1136/openhrt-2024-002642).

To cite: Minderhoud SCS, van Montfoort R, Meijs TA, *et al*. Aortic geometry and long-term outcome in patients with a repaired coarctation. *Open Heart* 2024;**11**:e002642. doi:10.1136/openhrt-2024-002642

SCSM and RvM contributed equally.

Received 9 April 2024
Accepted 15 May 2024

Check for updates

© Author(s) (or their employer(s)) 2024. Re-use permitted under CC BY-NC. No commercial re-use. See rights and permissions. Published by BMJ.

[1]Department of Cardiology, Erasmus Medical Center, Rotterdam, The Netherlands
[2]Department of Radiology, Erasmus Medical Center, Rotterdam, The Netherlands
[3]Department of Cardiology, University Medical Centre Utrecht, Utrecht, The Netherlands
[4]Vicomtech Foundation, Basque Research and Technology Alliance, Donostia-San Sebastián, Spain

Correspondence to
Dr Annemien E van den Bosch; a.e.vandenbosch@erasmusmc.nl

ABSTRACT

Objective This study aims to compare aortic morphology between repaired coarctation patients and controls, and to identify aortic morphological risk factors for hypertension and cardiovascular events (CVEs) in coarctation patients.

Methods Repaired coarctation patients with computed tomography angiography (CTA) or magnetic resonance angiography (MRA) were included, followed-up and compared with sex-matched and age-matched controls. Three-dimensional aortic shape was reconstructed using patients' CTA or MRA, or four-dimensional flow cardiovascular magnetic resonance in controls, and advanced geometrical characteristics were calculated and visualised using statistical shape modelling. In patients, we examined the association of geometrical characteristics with (1) baseline hypertension, using multivariable logistic regression; and (2) cardiovascular events (CVE, composite of aortic complications, coronary artery disease, ventricular arrhythmias, heart failure hospitalisation, stroke, transient ischaemic attacks and cardiovascular death), using multivariable Cox regression. The least absolute shrinkage and selection operator (LASSO) method selected the most informative multivariable model.

Results Sixty-five repaired coarctation patients (23 years (IQR 19–38)) were included, of which 44 (68%) patients were hypertensive at baseline. After a median follow-up of 8.7 years (IQR 4.8–15.4), 27 CVEs occurred in 20 patients. Aortic arch dimensions were smaller in patients compared with controls (diameter p<0.001, wall surface area p=0.026, volume p=0.007). Patients had more aortic arch torsion (p<0.001) and a higher curvature (p<0.001). No geometrical characteristics were associated with hypertension. LASSO selected left ventricular mass, male sex, tortuosity and age for the multivariable model. Left ventricular mass (p=0.014) was independently associated with CVE, and aortic tortuosity showed a trend towards significance (p=0.070).

Conclusion Repaired coarctation patients have a smaller aortic arch and a more tortuous course of the aorta compared with controls. Besides left ventricular mass index, geometrical features might be of importance in long-term risk assessment in coarctation patients.

WHAT IS ALREADY KNOWN ON THIS TOPIC

⇒ Patients with repaired coarctation of the aorta have a lifetime increased risk of developing cardiovascular events and hypertension, even without residual stenosis or re-coarctation.

⇒ Previous studies have shown that the distinct aortic geometry of coarctation patients may be associated with the increased risk of cardiovascular events; however, prospective studies evaluating the prognostic consequences of aortic geometry in this population are missing.

WHAT THIS STUDY ADDS

⇒ This study describes that repaired coarctation patients have a smaller aortic arch and a more tortuous course of the aorta compared with age-matched and sex-matched controls, stressing that in spite of successful repair, their aortic geometry is not similar compared with a normal aorta.

⇒ Aortic tortuosity was identified as a possible additional risk factor besides left ventricular mass and age.

HOW THIS STUDY MIGHT AFFECT RESEARCH, PRACTICE OR POLICY

⇒ Findings of this study suggest that aortic geometry deserves more attention in the follow-up of repaired coarctation patients, and especially patients with more aortic tortuosity might require closer surveillance.

⇒ Therefore, a large multicentre study is necessary to validate prognostic implications of aortic geometry in repaired coarctation patients.

INTRODUCTION

Surgical and percutaneous treatment of aortic coarctations is generally anatomically successfully relieved.[1] Despite effective repair, patients' life expectancy is diminished compared with the general population,[1 2] and patients have an increased risk of developing coronary artery disease, aortic complications, arrhythmias, heart failure and cerebrovascular events.[3]

Up to 57% of the patients have persistent or develop arterial hypertension, even without overt residual stenosis or re-coarctation.[1 4 5] Repaired aortas have abnormal vascular function, such as endothelial dysfunction, increased carotid intima-media thickness,

Open Heart: first published as 10.1136/openhrt-2024-002642 on 28 May 2024. Downloaded from http://openheart.bmj.com/ on June 26, 2024 at Utrecht University Library. Protected by copyright.

reduced arterial compliance, aortic stiffness, reduced baroreceptor sensitivity and dysregulation of the renin–angiotensin system, and this has been associated with surrogate endpoints such as hypertension and increased left ventricular (LV) mass.[6 7] Aortic shape has been related to both vascular dysfunction and LV ejection fraction, LV end-diastolic volume, LV mass and hypertension.[8–10]

We hypothesise that coarctation patients are at increased risk of cardiovascular morbidity and mortality because of their distinct aortic geometry and accompanied vascular dysfunction. This study aims (1) to describe a comprehensive method to analyse aortic geometry using current standard image protocols and state-of-the-art analytical techniques; (2) to compare aortic geometrical characteristics of repaired coarctation patients with healthy controls matched on sex and age; and (3) to investigate associations of geometrical features in repaired coarctation patients with hypertension and cardiovascular events (CVEs).

METHODS

Patient population

Patients with repaired coarctation (aged ≥18 years) from the Erasmus Medical Center registered in the prospective follow-up CONCOR registry were included when CT angiography (CTA) or magnetic resonance angiography (MRA) of the complete thoracic aorta within 5 years from inclusion was available (online supplemental figure 1). A post-hoc analysis was performed in patients with available imaging data of their thoracic aorta. Patients were included if they had either surgical or transcatheter repair of the aortic coarctation before their scan. Baseline characteristics including cardiovascular risk factors were collected at the time of inclusion in the registry. Hypertension was defined as a right brachial systolic blood pressure (SBP) >140 mm Hg, diastolic blood pressure (DBP) >90 mm Hg or prescription of antihypertensive medication, and was assessed at baseline and at follow-up.[11] LV mass was calculated using the Devereux formula based on echocardiographic reports and was indexed for body surface area. The degree of aortic valve regurgitation or stenosis was based on current guideline recommendations.[12 13] Atrial fibrillation was defined as described by treating specialist according to the European Society of Cardiology guidelines.[14] Patients were followed up for the occurrence of hypertension, reintervention of the coarctation and CVE from the time of the CTA/MRA until the last patient visit. CVE included aneurysms, dissections, coronary artery disease, ventricular arrhythmia, heart failure hospitalisation, cerebrovascular events, transient ischaemic attack and cardiovascular death. Definitions of CVE are described in the online supplemental appendix. Reinterventions included surgery, stenting, balloon angioplasty or a combination of the latter, aimed to relieve the residual or re-coarctation. CVEs occurring within 30 days from an invasive procedure were considered post-procedural and were excluded. CVEs were scored when reported by the treating physician. Healthy controls, without history of cardiovascular disease, were identified to describe aortic geometry differences between coarctation and the healthy population and were sex and age matched on a group level.

Image acquisition and segmentation

Scans were acquired between 2003 and 2018, on either Siemens CT scanner or GE MRI 1.5T scanner (figure 1). Follow-up scans were made to monitor aneurysm formation or ventricular function, evaluate residual or re-coarctation or for research purposes. Patients underwent the standard clinical aortic imaging protocol, including either CTA or MRA. Contrast-enhanced four-dimensional (4D) flow MRI was acquired in healthy controls following a standardised study protocol as reported previously.[15] Typical spatial resolution characteristics were 0.7×0.7×1.0 mm for CTA, 1.3×1.7×1.4 mm for MRA and 1.8×2.1×1.4 mm for 4D flow. Previously, excellent agreement was found between CTA and MRA-based aortic diameters in our institution.[16]

Three-dimensional geometry of the thoracic aorta and its branches was extracted from CTA or MRA using the semiautomated segmentation software ITK-snap (ITK-SNAP Medical Image Segmentation Tool) between the aortic annulus and the level of the diaphragm (figure 1). In healthy controls, a similar methodology was followed in CAAS MR Solutions V.5.1 (Pie Medical Imaging, Maastricht, the Netherlands) (figure 1). In Meshmixer (Autodesk, San Rafael, USA), the same aortic volume of interest was extracted, between the anatomical landmarks (annulus aortic valve and diaphragm), in all subjects (figure 1).

Geometry analysis

The global aortic arch geometry was visually categorised by two researchers (SCSM and RvM) into Romanesque, Crenel or Gothic (figure 2).[5] The type of coarctation was recorded based on surgical reports of the initial repair. The segmentations were processed using the Vascular Modeling Toolkit (VMTK, Orobix, Bergamo, Italy) (figure 1). The thoracic aorta was divided into the *ascending aorta* between the aortic valve annulus and the innominate artery, into the *aortic arch* between the innominate artery and the left subclavian artery and into the *descending aorta* between the left subclavian artery and the diaphragm. Mean aortic diameter, minimal luminal area, aortic wall surface area and volume of these segments were calculated using an in-house-developed Python script using VMTK functions. Segmentation of the descending aorta was incomplete in the healthy controls; consequently, all measurements of the descending aorta in this group were disregarded. The ratio between ascending and descending aortic diameter and percentage residual stenosis were derived from mean diameter measurements (figure 1A,B). The percentage residual stenosis was defined as $100 \times (1 - \text{diameter}_{\text{stenosis}} / \text{diameter}_{\text{reference}})$ in per cent. The average aortic diameter

Open Heart: first published as 10.1136/openhrt-2024-002642 on 28 May 2024. Downloaded from http://openheart.bmj.com/ on June 26, 2024 at Utrecht University Library. Protected by copyright.

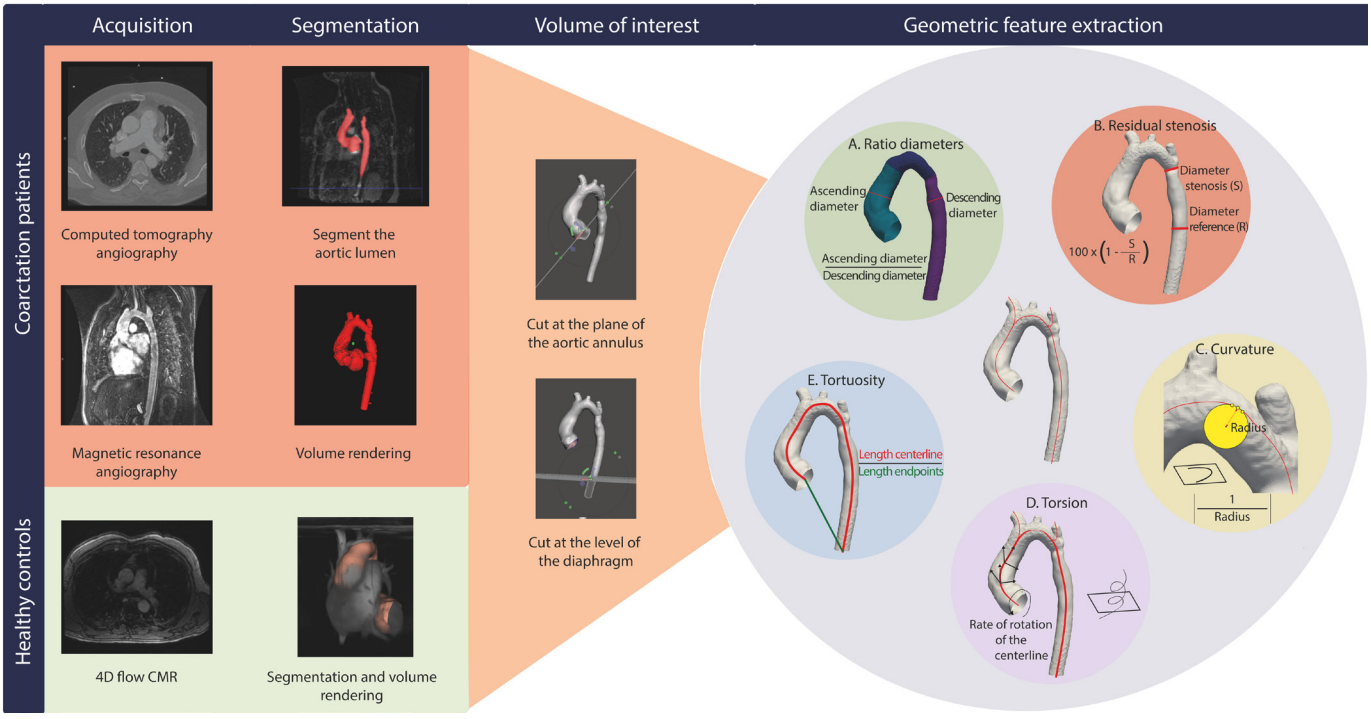

Figure 1 Workflow methodology. Aortic shapes were based on CT angiography, magnetic resonance angiography in patients and contrast-enhanced 4D flow CMR in healthy controls. Aortas were segmented and the volume of interest was between the aortic annulus and diaphragm. Using an in-house-developed Python script using VMTK functions, geometrical features were extracted. 4D, four-dimensional; CMR, cardiovascular magnetic resonance; VMTK, Vascular Modeling Toolkit.

of the descending aorta was taken as the reference diameter. Residual stenosis was considered significant if larger than 20%. Aortic arch was defined as hypoplastic when the ratio of the aortic arch diameter to the reference area in the descending aorta was smaller than 0.9.[17]

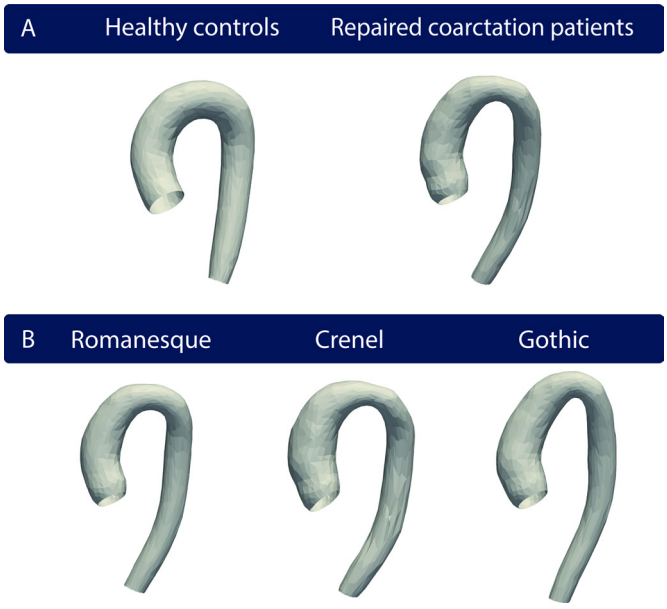

Figure 2 Average aortic shapes of subgroups. These are computed via SSM summarising the key shape features as associated with each group in three dimension (A) of healthy controls and repaired coarctation patients; (B) of patients with Romanesque-shaped, Crenel-shaped and Gothic-shaped aortic arches. SSM, statistical shape modelling.

The centreline of each aortic volume was determined and based on this centreline, the curvature, torsion and tortuosity of the centreline were calculated using VMTK functions (figure 1). The centreline is a curve and the deviation of a curve from linearity and planarity is described by the curvature and torsion. Curvature is the degree of bending of the centreline, the deviation from a straight line in one plane and was defined as the inverse of the radius of the osculating circle (figure 1C). The torsion is the twist of the centreline in space, the degree of deviation of the curve from the osculating plane (figure 1D). Curvature and torsion were calculated with the standard VMTK functions (*vmtkcenterlinegeometry*). Tortuosity was defined as the ratio of the centreline length and the direct distance between the centreline endpoints (figure 1E).

Average shape analysis via statistical shape modelling

In order to visualise the numerical results of our geometrical analysis and fully exploit three-dimensional shape information provided by the reconstructed aortic arches, average aortic shapes of subgroups of interest were calculated via statistical shape modelling (SSM).[9] The SSM method is a non-parametric method that analyses how a representative prototype shape (the template) deforms into each of the target shapes that are present in the population.

Open Heart: first published as 10.1136/openhrt-2024-002642 on 28 May 2024. Downloaded from http://openheart.bmj.com/ on June 26, 2024 at Utrecht University Library. Protected by copyright.

In short, of the healthy controls, the subject closest to the average volume, aortic wall surface area and centreline was chosen as the initial template. All aortas included for a subgroup were rigidly registered (i.e., aligned) to this initial template using the iterative closest point algorithm provided in VMTK. Average aortic shape (template) per group and its deformations towards each included subject shape were then calculated in the SSM framework Deformetrica (www.deformetrica.org), which used an alternate two-step minimisation algorithm.[18] First, the initial template is independently deformed towards each target shape in order to minimise the distance between deformed template and the respective target shapes with respect to the deformations. In the second step, a new, updated template is computed based on these deformations and the initial template in order to minimise the distance between the deformed template shapes (matched shapes) and the original target shapes with respect to the template.[19]

Once the template for a subgroup was computed, these steps were repeated with the newly calculated template aorta as initial template. This process was repeated until the final template, i.e. the final average aorta's shape did not change anymore following the principles of Generalised Procrustes Analysis.[20] The final template was assumed to be the average ('prototype') aortic shape, representative for the considered subgroup. As results are provided as three-dimensional computational surface meshes, this processing allows visualising a subgroup's average shape in three dimension comprising all relevant shape features instead of merely reporting average morphometric parameters.

Statistical analysis

Normality was visually checked on histograms. For continuous variables, mean and standard deviation (SD) in case of normal distribution, or median and the interquartile range (IQR (25th–75th)) in case of a non-normal distribution were calculated. Categorical variables were summarised with frequencies and percentages. Differences in baseline characteristics and geometrical measurements between patients and healthy controls were tested for significance using an unpaired t-test if normally distributed or a Mann-Whitney test if not normally distributed. To analyse differences of the original morphology, characteristics of the initial repair and geometrical characteristics between subgroups (descriptive morphology subtypes, tricuspid aortic valves (TAVs) vs bicuspid aortic valves (BAVs), surgical technique, no vs aortic hypoplasia), differences were tested with one-way analysis of variance (ANOVA) (when normally distributed) or Kruskal-Wallis test (when not normally distributed) and subsequently pairwise comparisons were performed between separate groups with an unpaired t-test or a Mann-Whitney test. For categorical variables, X^2 test or Fisher's exact test was performed, as appropriate. To determine the optimal cut-off value for the risk of hypertension and CVE, the Youden index was estimated at each percentage of residual stenosis and minimal luminal area of descending aorta and maximised.

To assess repeatability of our measurements, intraobserver variability of the geometrical measures was assessed in 15 randomly selected aortas (five CTA, five MRA and five 4D flow MRI). Repeatability data were reported using intraclass correlation coefficients (ICCs). The ICC was calculated using a two-way ANOVA model to determine observer variability based on a single measure and absolute agreement.

Univariable logistic regressions were used to investigate the association between the type of coarctation and presence of hypoplasia, characteristics of the initial repair (type of surgery and age at initial surgery) and baseline and geometrical characteristics with hypertension at the baseline moment. Univariable Cox proportional hazard regressions were used to investigate determinants of CVE and reintervention. Patients were followed from the time of the scan until the occurrence of a CVE and reintervention. If no CVE or reintervention occurred, they were censored at the time of the last clinic visit. For these analyses, residual stenosis was entered as a continuous variable. To obtain the most informative multivariable logistic regression and Cox proportional hazards models, while also considering the limited number of events per variable, we applied least absolute shrinkage and selection operator (LASSO) penalised regression with the penalty parameter selected by 10-fold cross-validation. Besides the geometrical risk factors, other risk factors were included based on their clinical relevance and previous reports; these included sex, age at inclusion, age at repair, aortic valve type, type of surgery and LV mass indexed.[2]

Statistical analyses were conducted using R Statistical Software V.4.1.0 (R Foundation for Statistical Computing, Vienna, Austria). Two-tailed p values of <0.05 were considered statistically significant.

RESULTS

Study population

In total, 65 patients were eligible for inclusion. Baseline variables of patients and healthy controls are shown in table 1. Fourteen patients had aortic arch hypoplasia, of which the majority (10 out of 14) had proximal aortic arch hypoplasia. Other than SBP, no differences were statistically significant. Time between inclusion and scan was 1.6 years (IQR 0.5–3.0). During the follow-up between CTA/MRA until censoring (median 8.7 years (IQR 4.8–15.4)), 27 CVEs occurred in 20 patients. Four patients died because of a cardiovascular reason, and aortic aneurysm was the most frequently occurring event (22%, 6 of 27 times) (online supplemental table 1). Five of the six aneurysms occurred in the ascending aortic in patients with a BAV and not at the site of the surgical repair. Four (6%) patients went for reintervention during follow-up at a median follow-up period of 1.2 years (IQR 0.6–1.7). Given the low number of reinterventions, no further univariable and multivariable analyses were performed

Open Heart: first published as 10.1136/openhrt-2024-002642 on 28 May 2024. Downloaded from http://openheart.bmj.com/ on June 26, 2024 at Utrecht University Library. Protected by copyright.

Table 1 Baseline characteristics

	Healthy controls (n=23)	Coarctation patients (n=65)	P value*
Age (years)	30 (26–34)	23 (19–38)	0.119
Male sex	11 (48%)	36 (55%)	0.538
Weight (kg)	71 (65–83)	75 (64–89)	0.662
Height (cm)	178 (174–185)	174 (164–183)	0.056
Systolic blood pressure (mm Hg)	110 (103–115)	140 (125–151)	<0.001
Diastolic blood pressure (mm Hg)	67 (64–74)	77 (67–85)	0.002
Hypertension	–	44 (68%)	–
Smoking	–	13 (20%)†	–
Hypercholesterolaemia	–	6 (9%)	–
Diabetes mellitus	–	3 (5%)	–
Atrial fibrillation/atrial flutter	–	5 (8%)	–
Bicuspid aortic valve morphology	–	49 (75%)	–
Aortic valve stenosis (≥moderate)	–	8 (12%)	–
Aortic valve regurgitation (≥moderate)	–	5 (8%)	–
Left ventricular mass indexed (g/m^2)	79 (66–89)	82 (70–106)	0.149
Age at initial repair (years)	–	4.8 (0.1–14.2)	–
Type of coarctation			
Pre-ductal	–	7 (11%)	–
Juxta-ductal	–	47 (72%)	–
Post-ductal	–	11 (17%)	–
Hypoplastic aortic arch	–	14 (22%)	–
Type of surgery			
End-to-end anastomosis	–	46 (71%)	–
Patch angioplasty	–	9 (14%)	–
Subclavian flap aortoplasty	–	6 (9%)	–
Interposition graft	–	2 (3%)	–
Bypass	–	1 (2%)	–
Percutaneous stenting	–	1 (2%)	–
Follow-up period (years)	–	8.7 (4.8–15.4)	–

Median with IQR, or number with percentage.
*Comparing healthy controls with coarctation patients.
†Of three patients, smoking data were missing.

on risk factors of reinterventions. At the last clinical visit, 45 (69%) patients had hypertension or antihypertensive medication (of which 40 used antihypertensive medication) and the median blood pressure was 132/79 mm Hg. Comparing baseline versus follow-up, SBP decreased (p=0.045), DBP was similar (p=0.357), antihypertensive medication increased (p=0.036) and overall patients with hypertension was similar (p=0.853). Patients were matched with 23 healthy controls.

Aortic geometry

An overview of the aortic geometry parameters in healthy controls and coarctation patients is presented in table 2 and is visually reflected in figure 2A. Ascending aortic diameters, wall surface area and volume were not different in coarctation patients with a TAV compared with healthy controls, but were higher in coarctation patients with a BAV compared with healthy controls (all p<0.001) (table 2). Aortic arch diameters, wall surface area and volumes were smaller in coarctation patients compared with healthy controls (diameter p<0.001, wall surface area p=0.026 and volume p=0.007). Patients had more torsion of their thoracic aorta (entire thoracic aorta patients 30 dm^{-1} (IQR 27–33), healthy controls 22 dm^{-1} (IQR 20–25; p<0.001); aortic arch patients 17 dm^{-1} (IQR 11–21), healthy controls 10 dm^{-1} (IQR 8–13; p<0.001)) (table 2 and figure 2). The aortic arch curvature was

Open Heart: first published as 10.1136/openhrt-2024-002642 on 28 May 2024. Downloaded from http://openheart.bmj.com/ on June 26, 2024 at Utrecht University Library. Protected by copyright.

Table 2 Geometrical characteristics

	Healthy controls (n=23)	Repaired coarctation patients (n=65)		Beta (95% CI), p value*	
Aortic geometry (n, %)				–	
Romanesque	23 (100)	33 (51)			
Gothic	0 (0)	24 (35)			
Crenel	0 (0)	8 (12)			
Ascending aorta		TAV	BAV	†	‡
Diameter (mm)	28 (26–29)	28 (26–31)	32 (28–36)	0 (–2, 3), 0.746	4 (2, 6), <0.001
Wall surface area (cm^2)	73 (43–80)	81 (63–88)	104 (86–138)	7 (–4, 19), 0.263	35 (22, 54), <0.001
Volume (cm^3)	40 (34–49)	48 (34–56)	67 (53–102)	5 (–5, 15), 0.315	30 (18, 50), <0.001
Ratio ascending–descending diameter	–	2.1 (1.7–2.5)	2.3 (2.0–2.9)	–	–
Aortic arch					
Diameter (mm)	26 (24–26)	21 (19–24)		–4 (–5, –2), <0.001	
Wall surface area (cm^2)	47 (42–52)	41 (33–52)		–6 (–12, –1), 0.026	
Volume (cm^3)	23 (20–25)	16 (11–25)		–6 (–10, –2), 0.007	
Descending aorta					
Diameter (mm)	–	20 (18–24)		–1 (–3, 1), 0.146	
Wall surface area (cm^2)	–	111 (84–149)		–	
Volume (cm^3)	–	54 (35–86)		–	
Residual stenosis (%)	–	14 (0–28)		–	
Residual stenosis >20% (n)	–	26 (40%)		–	
Minimal luminal area descending aorta (mm^2)	294 (258–358)	210 (130–274)		–95 (–141, –52), <0.001	
Aortic tortuosity	–	2.3 (2.0–2.7)		–	
Mean torsion aortic arch (dm^{-1})	10 (8–13)	17 (11–21)		5.3 (0.3, 8.2), <0.001	
Mean aortic arch curvature (dm^{-1})	3.7 (3.4–4.0)	4.2 (3.8–4.9)		0.6 (0.3, 1.0), <0.001	

Median with IQR, or number with percentage. As in healthy controls, not the complete descending aorta was available in all subjects, descending aortic wall surface area, volume and tortuosity could not be calculated.
*P value comparing healthy controls with coarctation patients.
†P value comparing healthy controls with coarctation patients with a TAV.
‡P value comparing healthy controls with coarctation patients with a BAV.
BAV, bicuspid aortic valve; TAV, tricuspid aortic valve.

significantly higher in patients (4.2 dm^{-1} (IQR 3.8–4.9)) compared with healthy controls (3.7 dm^{-1} (IQR 3.4–4.0); p<0.001).

Differences stratified per descriptive aortic morphology are presented in online supplemental table 2 and figure 2B. Patients with a Crenel-shaped aorta were significantly older at their initial intervention (p=0.046) and had more commonly a hypoplastic aortic arch (p=0.007) compared with patients with a Romanesque-shaped aorta. LV mass indexed was higher in patients with a Gothic-shaped aorta compared with Romanesque-shaped aortas (p=0.023). Aortic torsion was higher in patients with a Gothic-shaped aorta compared with Crenel (p=0.008) or Romanesque-shaped aortas (p=0.022), and aortic arch torsion was lower in patients with a Romanesque-shaped aorta (vs Crenel p=0.027, vs Gothic p=0.010). Aortic arch hypoplasia was not significantly different in geometry groups. No other clinical or geometrical parameters were associated with a certain aortic arch morphology.

Besides larger aortic arch wall surface and volume in patients with BAV, there were no geometrical differences between patients with a BAV and a TAV (online supplemental table 3). Online supplemental table 4 shows the analysis of aortic shape features of the three most common surgical techniques in our cohort. Patients with a patch angioplasty were significantly older, had a higher LV mass, more residual stenosis and more torsion of their aortic arch compared with end-to-end anastomosis patients. Finally, the aortic shape was compared of patients with and without hypoplastic aortic arches (online supplemental table 5). Patients with hypoplastic aortic arches were more often hypertensive and had significantly more tortuosity and a lower mean aortic arch curvature compared with those without aortic arch hypoplasia.

Intraobserver agreement of the aortic shape metrics was in general good to excellent (online supplemental table 6), except for the aortic arch volume (ICC 0.789 (95% CI 0.493 to 0.923)) and aortic torsion (ICC 0.530 (95% 0.057 to 0.812)) (online supplemental table 6).

Open Heart: first published as 10.1136/openhrt-2024-002642 on 28 May 2024. Downloaded from http://openheart.bmj.com/ on June 26, 2024 at Utrecht University Library. Protected by copyright.

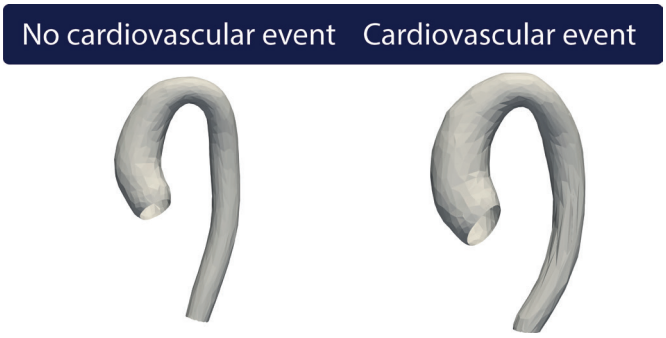

Figure 3 Average aortic shapes of patients with and without cardiovascular event. These are computed via SSM summarising the key shape features as associated with patients with and without cardiovascular event in three dimension. Patients without cardiovascular events have a more Romanesque-shaped aorta, while patients with cardiovascular events have a more angulated aortic arch and tortuous course of the descending aorta. SSM, statistical shape modelling.

Risk factors for hypertension

In univariable logistic regression, male sex, age, age at repair, LV mass indexed and aortic arch hypoplasia were positively associated with hypertension (male sex OR 1.33 (95% CI 1.07 to 1.66), p=0.013; age per 5-year increase OR 1.05 (95% CI 1.01 to 1.10), p=0.025; age at repair per 5 years OR 1.11 (95% CI 1.05 to 1.17), p<0.001; LV mass indexed per 25 g/m^2 (LV mass) OR 1.08 (95% CI 1.01 to 1.16); and hypoplastic aortic arch 1.29 (95% CI 1.00 to 1.66), p=0.023) (online supplemental table 7). After LASSO regression selection, in the most informative multivariable model, male sex, age per 5 years and tortuosity were associated with hypertension. Based on the highest Youden index, the optimal cut-off value for a residual stenosis was 25% to distinguish patients with and without hypertension (Youden index 0.20). For the minimal luminal area, 134 mm^2 was the optimal cut-off value.

Risk factors of CVEs

Figure 3 shows the average aortic shape of patients with and without CVE. Patients without CVE had a Romanesque-shaped aorta more similar to the aortic shape of healthy controls, while patients with CVE had a more angulated aortic arch and a more tortuous course of the descending aorta. Based on the highest Youden index, the optimal cut-off value for a residual stenosis was 15% to distinguish patients with and without CVE (Youden index 0.11). Online supplemental table 8 shows regression analysis of risk factors for CVE. In the univariable analysis of the geometrical features, aortic tortuosity and minimal luminal area of the descending aorta were associated with increased risk of CVE (aortic tortuosity HR 2.20 (95% CI 1.18 to 4.10), p=0.013; and minimal luminal area of the descending aorta HR 1.00 (95% CI 1.00 to 1.01), p=0.035). Residual stenosis was not associated with CVE. Using LASSO, age, LV mass and aortic tortuosity were selected for the most informative multivariable model. In this model, LV mass was independently associated with CVE (HR 1.38 (95% CI 1.07 to 1.78), p=0.014). There was a trend towards an association between aortic tortuosity and CVE; however, this was not significant (HR for aortic tortuosity 2.20 (95% CI 0.94 to 5.17), p=0.070) (online supplemental table 8).

DISCUSSION

The current study shows that comprehensive analysis of three-dimensional geometrical features of the aorta is feasible using standard imaging protocols and state-of-the-art analysis techniques such as SSM. Geometrical aortic characteristics of coarctation patients (with and without CVE) and healthy age-matched controls were quantitatively compared and visually summarised via computed three-dimensional average shapes. Residual stenosis was not associated with the occurrence of CVE, while there was a trend towards an association between aortic tortuosity and CVE.

The presented methodology provides a complete overview of the aortic geometry in coarctation patients by looking beyond simple aortic dimensions, and investigate for example, cross-sectional vessel area, wall surface area and volumes. With three-dimensional metrics, such as the curvature and torsion, the course of the aorta through the thorax is quantified. This study demonstrates that the aorta of coarctation patients has a distinct shape and a more complex course compared with the healthy population with more torsion, a higher curvature and a smaller aortic arch. These differences underline that coarctation of the aorta is not just a 'narrowing' at the aortic isthmus, but an aortopathy affecting a larger region of the aorta.

No studies have reported the relationship between complex aortic shape features and CVE. In other patient groups, i.e., patients with Marfan syndrome, ascending aortic curvature was associated with thoracic aneurysm growth.[21] Previous studies in coarctation patients associated a more curved, Gothic-shaped aortic arch with surrogate endpoints such as cardiac parameters (e.g., lower LV ejection fraction) and vascular parameters (e.g., abnormal intima thickness).[8 9] In this study, although aortic arch curvature appeared to be higher in patients with CVE, there was no significant association between curvature and/or Gothic-shaped aorta and CVE. As in a previous study in patients with a type B aortic dissection, tortuosity was associated with CVE in this study which might be a stronger predictor than curvature and/or Gothic-shaped aorta.[22]

Interplay between aortic shape, flow and pathophysiology has long been recognised both in embryology, vessel homeostasis and in the onset of disease.[23 24] In coronary arteries, vessel torsion specifically has shown to promote helical flow.[25] Helical flow is associated with higher wall shear stress values and is considered atheroprotective, but also with plaque rupture and aneurysm formation.[15 26–29] Pathological wave reflections were previously associated with aortic radius and not with curvature.[30]

Open Heart: first published as 10.1136/openhrt-2024-002642 on 28 May 2024. Downloaded from http://openheart.bmj.com/ on June 26, 2024 at Utrecht University Library. Protected by copyright.

In our population, potentially altered haemodynamics, because of the altered vessel shape, impact the aortic wall by inducing vessel wall remodelling and increasing LV afterload. These two processes are associated with the occurrence of CVE. However, the assessment of the direct relationship between altered flow haemodynamics and the risk on CVE was beyond the scope of this research.

For the risk of hypertension, a cut-off for a residual stenosis of 25% narrowing of the aortic diameter seems to be appropriate and the minimal luminal area in the descending aorta was not better to predict hypertension than the degree of residual stenosis. The low Youden index of both parameters supports the theory that other factors (e.g., vascular remodelling) play an important role in the development of hypertension.[8] Clinical parameters such as male sex and age at repair appeared to have stronger associations with hypertension than residual stenosis and arch curvature. The degree of residual stenosis is currently central in the treatment of repaired coarctation patients, is associated with LV afterload and aortic wall shear stresses proximal to the coarctation and was expected to predict the risk of CVE.[31 32] However, the present study did not show an association between the degree of residual stenosis and the risk on CVE. The low Youden index of residual stenosis also stresses that the predictive value of residual stenosis for CVE is not strong. Future larger studies are required to confirm this finding.

Study limitations

For aortic shape reconstructions, different imaging modalities were used for coarctation patients and controls which might have impacted the aortic dimension measurements and hindered the evaluation of features involving the distal descending aorta in controls. Only patients with a CT or MRI available acquired in a certain time frame were selected and this might have resulted in inclusion of a selected population; the results might not be applicable to all postoperative coarctation patients. Despite LASSO penalised regression, there is a possibility that our multivariable models are influenced by characteristics unique to our small sample size. Also, our study population was rather small and the total number of events was small. Therefore, our findings should be confirmed in larger studies. Finally, ambulatory blood pressure measurements were not available in all patients; therefore, office blood pressure measurements were used.

CONCLUSION

After successful coarctation repair, patients have a distinct aortic arch geometry compared with matched controls with a more tortuous course and smaller aortic arch. The degree of residual stenosis can only partly explain the presence of hypertension in patients and was not associated with CVE. However, to predict CVE, other geometrical features (e.g., tortuosity) might be helpful. Gaining insight into which factors attribute to the altered aortic morphology in coarctation patients may be beneficial in reducing lifelong cardiovascular burden in these patients and improving their quality of life.

Contributors Conceptualisation—SCSM, RvM, TAM, MV and AEvdB. Data curation—SCSM, RvM and TAM. Data processing—S-AK. Formal analysis—SCSM and RvM. Supervision—AEvdB. Writing (original draft)—SCSM, RvM and AEvdB. Writing (review and editing)—all authors. Guarantor—SCSM.

Funding This research was funded by the Thorax Foundation.

Competing interests None declared.

Patient consent for publication Not applicable.

Ethics approval This study involves human participants and was approved by the Erasmus Medical Center Ethical Committee (MEC-2019-0664). All participating patients provided written informed consent.

Provenance and peer review Not commissioned; externally peer reviewed.

Data availability statement Data are available upon reasonable request.

Supplemental material This content has been supplied by the author(s). It has not been vetted by BMJ Publishing Group Limited (BMJ) and may not have been peer-reviewed. Any opinions or recommendations discussed are solely those of the author(s) and are not endorsed by BMJ. BMJ disclaims all liability and responsibility arising from any reliance placed on the content. Where the content includes any translated material, BMJ does not warrant the accuracy and reliability of the translations (including but not limited to local regulations, clinical guidelines, terminology, drug names and drug dosages), and is not responsible for any error and/or omissions arising from translation and adaptation or otherwise.

Open access This is an open access article distributed in accordance with the Creative Commons Attribution Non Commercial (CC BY-NC 4.0) license, which permits others to distribute, remix, adapt, build upon this work non-commercially, and license their derivative works on different terms, provided the original work is properly cited, appropriate credit is given, any changes made indicated, and the use is non-commercial. See: http://creativecommons.org/licenses/by-nc/4.0/.

ORCID iDs
Alexander Hirsch http://orcid.org/0000-0002-3315-2006
Jolien W Roos-Hesselink http://orcid.org/0000-0002-6770-3830
Annemien E van den Bosch http://orcid.org/0000-0002-0422-9860

REFERENCES

1 Brown ML, Burkhart HM, Connolly HM, *et al*. Coarctation of the aorta: lifelong surveillance is mandatory following surgical repair. *J Am Coll Cardiol* 2013;62:1020–5.
2 Meijs TA, Minderhoud SCS, Muller SA, *et al*. Cardiovascular morbidity and mortality in adult patients with repaired aortic coarctation. *J Am Heart Assoc* 2021;10:e023199.
3 Cohen M, Fuster V, Steele PM, *et al*. Coarctation of the aorta long-term follow-up and prediction of outcome after surgical correction. *Circulation* 1989;80:840–5.
4 Nanton MA, Olley PM. Residual hypertension after coarctectomy in children. *Am J Cardiol* 1976;37:769–72.
5 Ou P, Bonnet D, Auriacombe L, *et al*. Late systemic hypertension and aortic arch geometry after successful repair of coarctation of the aorta. *Eur Heart J* 2004;25:1853–9.
6 Meyer AA, Joharchi MS, Kundt G, *et al*. Predicting the risk of early atherosclerotic disease development in children after repair of aortic coarctation. *Eur Heart J* 2005;26:617–22.
7 de Divitiis M, Pilla C, Kattenhorn M, *et al*. Ambulatory blood pressure, left ventricular mass, and conduit artery function late after successful repair of coarctation of the aorta. *J Am Coll Cardiol* 2003;41:2259–65.
8 Ou P, Celermajer DS, Mousseaux E, *et al*. Vascular remodeling after "successful" repair of coarctation. impact of aortic arch geometry. *J Am Coll Cardiol* 2007;49:883–90.
9 Bruse JL, Khushnood A, McLeod K, *et al*. How successful is successful? Aortic arch shape after successful aortic coarctation repair correlates with left ventricular function. *J Thorac Cardiovasc Surg* 2017;153:418–27.
10 Lee MGY, Kowalski R, Galati JC, *et al*. Twenty-four-hour ambulatory blood pressure monitoring detects a high prevalence of hypertension late after coarctation repair in patients with hypoplastic arches. *J Thorac Cardiovasc Surg* 2012;144:1110–6.

Open Heart: first published as 10.1136/openhrt-2024-002642 on 28 May 2024. Downloaded from http://openheart.bmj.com/ on June 26, 2024 at Utrecht University Library. Protected by copyright.

11 Williams B, Mancia G, Spiering W, *et al*. 2018 ESC/ESH guidelines for the management of arterial hypertension. *Eur Heart J* 2018;39:3021–104.
12 Baumgartner H, Hung J, Bermejo J, *et al*. Recommendations on the echocardiographic assessment of aortic valve stenosis: a focused update from the European association of cardiovascular imaging and the American society of echocardiography. *J Am Soc Echocardiogr* 2017;30:372–92.
13 Zoghbi WA, Adams D, Bonow RO, *et al*. Recommendations for noninvasive evaluation of native valvular regurgitation a report from the American society of echocardiography developed in collaboration with the society for cardiovascular magnetic resonance. *J Am Soc Echocardiogr* 2017;30:303–71.
14 Hindricks G, Potpara T, Dagres N, *et al*. 2020 ESC guidelines for the diagnosis and management of atrial fibrillation developed in collaboration with the European association for cardio-thoracic surgery (EACTS). *Eur Heart J* 2021;42:373–498.
15 Minderhoud SCS, Roos-Hesselink JW, Chelu RG, *et al*. Wall shear stress angle is associated with aortic growth in bicuspid aortic valve patients. *Eur Heart J Cardiovasc Imaging* 2022;23:1680–9.
16 Bons LR, Duijnhouwer AL, Boccalini S, *et al*. Intermodality variation of aortic dimensions: how, where and when to measure the ascending aorta. *Int J Cardiol* 2019;276:230–5.
17 Bogaert J, Kuzo R, Dymarkowski S, *et al*. Follow-up of patients with previous treatment for coarctation of the thoracic aorta: comparison between contrast-enhanced MR angiography and fast spin-echo MR imaging. *Eur Radiol* 2000;10:1847–54.
18 Mansi T, Voigt I, Leonardi B, *et al*. A statistical model for quantification and prediction of cardiac remodelling: application to tetralogy of fallot. *IEEE Trans Med Imaging* 2011;30:1605–16.
19 Durrleman S, Prastawa M, Charon N, *et al*. Morphometry of anatomical shape complexes with dense deformations and sparse parameters. *NeuroImage* 2014;101:35–49.
20 Heimann T, Meinzer HP. Statistical shape models for 3d medical image segmentation: a review. *Med Image Anal* 2009;13:543–63.
21 van Hout MJP, Juffermans JF, Lamb HJ, *et al*. Ascending aorta curvature and flow displacement are associated with accelerated aortic growth at long-term follow-up: a MRI study in Marfan and thoracic aortic aneurysm patients. *Int J Cardiol Heart Vasc* 2022;38:100926.
22 Shirali AS, Bischoff MS, Lin H-M, *et al*. Predicting the risk for acute type B aortic dissection in hypertensive patients using anatomic variables. *JACC Cardiovasc Imaging* 2013;6:349–57.
23 Wang Y, Dur O, Patrick MJ, *et al*. Aortic arch morphogenesis and flow modeling in the chick embryo. *Ann Biomed Eng* 2009;37:1069–81.
24 Sotelo J, Valverde I, Martins D, *et al*. Impact of aortic arch curvature in flow haemodynamics in patients with transposition of the great arteries after arterial switch operation. *Eur Heart J Cardiovasc Imaging* 2022;23:402–11.
25 De Nisco G, Kok AM, Chiastra C, *et al*. The atheroprotective nature of helical flow in coronary arteries. *Ann Biomed Eng* 2019;47:425–38.
26 De Nisco G, Hoogendoorn A, Chiastra C, *et al*. The impact of helical flow on coronary atherosclerotic plaque development. *Atherosclerosis* 2020;300:39–46.
27 Liu X, Pu F, Fan Y, *et al*. A numerical study on the flow of blood and the transport of LDL in the human aorta: the physiological significance of the helical flow in the aortic arch. *Am J Physiol Heart Circ Physiol* 2009;297:H163–70.
28 Fukumoto Y, Hiro T, Fujii T, *et al*. Localized elevation of shear stress is related to coronary plaque rupture. A 3-dimensional Intravascular ultrasound study with in-vivo color mapping of shear stress distribution. *J Am Coll Cardiol* 2008;51:645–50.
29 Guala A, Dux-Santoy L, Teixido-Tura G, *et al*. Wall shear stress predicts aortic dilation in patients with bicuspid aortic valve. *JACC Cardiovasc Imaging* 2022;15:46–56.
30 Quail MA, Segers P, Steeden JA, *et al*. The aorta after coarctation repair - effects of calibre and curvature on arterial haemodynamics. *J Cardiovasc Magn Reson* 2019;21:22.
31 Baumgartner H, De Backer J, Babu-Narayan SV, *et al*. 2020 ESC guidelines for the management of adult congenital heart disease. *Eur Heart J* 2021;42:563–645.
32 Rafieianzab D, Abazari MA, Soltani M, *et al*. The effect of Coarctation degrees on Wall shear stress indices. *Sci Rep* 2021;11:1–13.

Open Heart: first published as 10.1136/openhrt-2024-002642 on 28 May 2024. Downloaded from http://openheart.bmj.com/ on June 26, 2024 at Utrecht University Library. Protected by copyright.

Supplemental Material

Supplemental Appendix: definitions cardiovascular events

Aortic aneurysm was defined as a 50% diameter increase to the expected diameter based on the thoracic aortic segment and sex and/or requiring surgical treatment(1). A dissection included aortic dissection, but also pseudoaneurysm, intramural hematoma, and rupture of the thoracic aorta. Coronary artery disease consisted of myocardial infarction and coronary revascularization. Ventricular arrhythmias comprised ventricular fibrillation/flutter (if survived) and sustained and non-sustained ventricular tachycardia. Non-sustained ventricular tachycardia was only scored as a CVE when subsequent medical or device treatments was initiated. Heart failure hospitalizations comprised an unscheduled hospital admission for a primary diagnosis of heart failure with a length of stay that either exceeds 24 h or crosses a calendar day. Cerebrovascular events and transient ischemic attack events were identified as radiologically confirmed bleeding or infarct reported by a radiologist, or a clinical diagnosis and classification of stroke recorded by the attending physicians. Cardiovascular death was defined as death resulting from an acute myocardial infarction (MI), sudden cardiac death, death due to heart failure (HF), death due to stroke, death due to cardiovascular (CV) procedures, death due to CV hemorrhage, and death due to other CV causes(2).

Supplemental Figure 1: Study population Flow Diagram

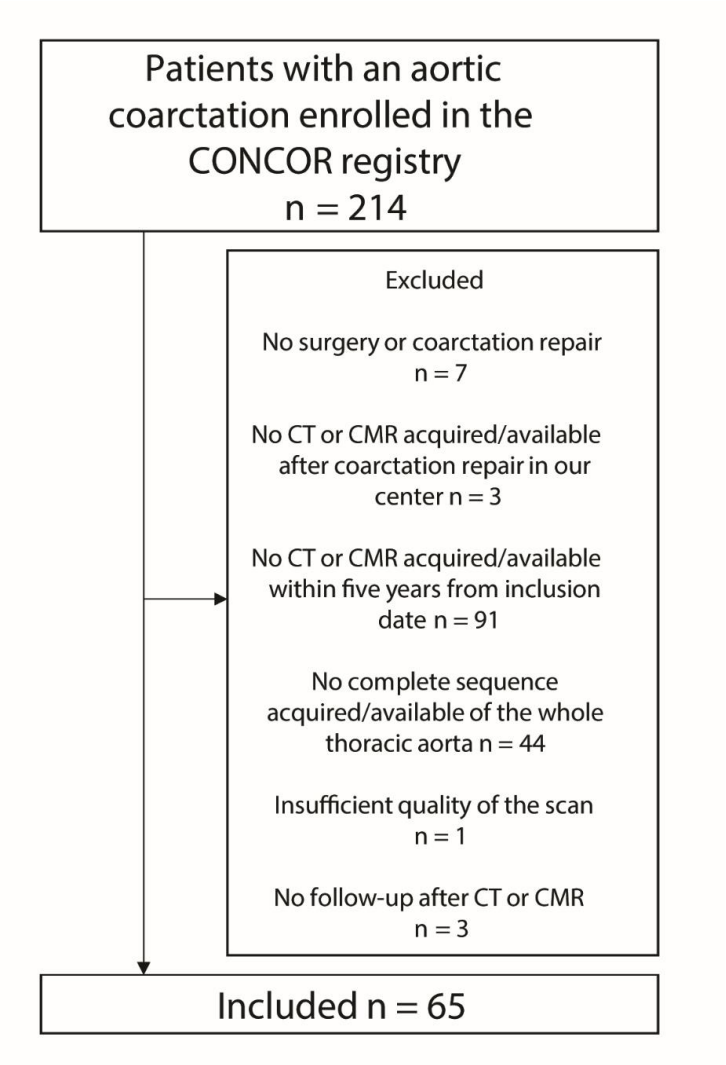

Supplemental table 1 cardiovascular events	
Aortic aneurysm	6 (9%)
Aortic dissection	3 (5%)
Coronary artery disease	2 (3%)
Heart failure hospitalization	4 (6%)
Stroke	2 (3%)
Transient ischemic attack	4 (6%)
Ventricular arrhythmia	2 (3%)
Cardiovascular death	4 (6%)
Total number of CVE	27
No. of individual patients with CVE[a]	20 (31%)
Number with percentage of the total number of patients; [a] number of patients with ≥1 event. CVE = cardiovascular events.	

Supplemental table 2 characteristics at baseline per descriptive morphology type						
	Romanesque	**Crenel**	**Gothic**	P-value[a]	P-value[b]	P-value[c]
	(n=33)	**(n=8)**	**(n=24)**			
Age at initial repair (years)	4.8 (0.1-10.7)	13.5 (7.4-18.4)	4.5 (0.1-8.3)	0.046	0.981	0.055
Type of coarctation				1.000	0.594	0.768
Pre-ductal	3 (9%)	0 (0%)	4 (17%)			
Juxta-ductal	23 (70%)	7 (88%)	17 (71%)			
Post-ductal	7 (21%)	1 (13%)	3 (13%)			
Hypoplastic aortic arch	3 (9%)	4 (50%)	7 (29%)	0.007	0.053	0.303
Aortic arch						
Diameter (mm)	21 (19-24)	21 (20-22)	22 (20-25)	0.735	0.417	0.380
Wall surface area (cm^2)	40 (31-50)	40 (36-44)	42 (34-53)	0.936	0.485	0.654
Volume (cm^3)	19 (10–23)	14 (12-16)	17 (11-32)	0.572	0.547	0.404
Hypertension	21 (64%)	7 (100%)	16 (67%)	0.206	0.822	0.276
Left ventricular mass indexed (g/m^2)	77 (66-102)	107 (80-153)	101 (80-128)	0.146	0.036	0.815
Residual stenosis (%)	12 (0-28)	15 (3-34)	17 (2-27)	0.630	0.696	0.913
Aortic tortuosity	2.4 (2.0-2.7)	2.3 (2.1-3.0)	2.2 (1.9-2.8)	0.717	0.482	0.528
Mean torsion aortic arch (dm^{-1})	14 (9-18)	21 (16-22)	19 (15-22)	0.027	0.010	0.685
Mean aortic arch curvature (dm^{-1})	4.0 (3.8-4.8)	4.3 (3.9-4.8)	4.4 (3.9-5.1)	0.755	0.361	0.862
Median with interquartile range, or number with percentage. [a]Romanesque vs Crenel, [b]Romanesque vs Gothic, [c]Crenel vs Gothic.						

Supplemental table 3 characteristics at baseline per aortic valve type			
	Tricuspid aortic valve	**Bicuspid aortic valve**	**P-value** [a]
	(n=16)	**(n=49)**	
Age at initial repair (years)	2.3 (0-11.5)	5.4 (0.3-14.9)	0.252
Hypoplastic aortic arch	3 (19%)	11 (22%)	0.765
Aortic arch			
Diameter (mm)	21 (18-23)	22 (19-25)	0.307
Wall surface area (cm^2)	33 (29-41)	42 (36-55)[a]	0.012
Volume (cm^3)	12 (8-18)	19 (12-29)[a]	0.034
Hypertension	9 (56%)	35 (71%)	0.267
Left ventricular mass indexed (g/m^2)	88 (69-98)	80 (71-107)	0.603
Residual stenosis (%)	20 (6-28)	13 (0-28)	0.395
Aortic tortuosity	2.1 (1.9-2.4)	2.4 (2.0-2.9)	0.110
Mean torsion aortic arch (dm^{-1})	19 14-24)	17 (11-20)	0.131
Mean aortic arch curvature (dm^{-1})	4.1 (3.9-4.7)	4.2 (3.8-5.1)	0.885
Median with interquartile range, or number with percentage. [a]Tricuspid vs bicuspid aortic valve.			

Supplemental table 4 characteristics at baseline per surgical technique						
	End to end anastomosis (n=46)	**Patch angioplasty (n=9)**	**Subclavian flap aortoplasty (n=6)**	**P-value** [a]	**P-value** [b]	**P-value**[c]
Age at initial repair (years)	4.8 (0.1-10.7)	14.9 (4.2-17)[a]	1.4 (0.0-2.3)[c]	0.029	0.707	0.007
Hypoplastic aortic arch	8 (17%)	2 (22%)	3 (50%)	0.655	0.121	0.277
Aortic arch						
Diameter (mm)	21 (19-25)	22 (21-22)	22 (18-22)	0.581	0.728	0.368
Wall surface area (cm^2)	41 (34-52)	38 (37-48)	33 (31-54)	0.864	0.696	0.765
Volume (cm^3)	17 (11–29)	13 (11-23)	15 (11-19)	0.645	0.562	0.831
Hypertension	31 (67%)	6 (67%)	4 (67%)	0.910	0.884	0.957
Left ventricular mass indexed (g/m^2)	76 (67-104)	101 (88-114)[a]	71 (65-95)	0.006	0.466	0.072
Residual stenosis (%)	13 (0-26)	20 (4-37)[a]	19 (12-33)[b]	0.032	0.035	0.726
Aortic tortuosity	2.3 (1.9-2.7)	2.4 (2.1-2.7)	2.4 (2.0-3.5)	0.855	0.646	0.521
Mean torsion aortic arch (dm^{-1})	15 (10-20)	22 (13-22)[a]	17 (14-20)	0.048	0.315	0.282
Mean aortic arch curvature (dm^{-1})	4.3 (3.8-5.0)	4.1 (4.0-4.5)	4.1 (3.2-5.2)	0.934	0.992	0.758
Median with interquartile range, or number with percentage. [a] End to end anastomosis vs patch angioplasty, [b] end to end anastomosis vs subclavian flap aortoplasty, [c]patch angioplasty vs subclavian flap aortoplasty.						

Supplemental table 5 characteristics at baseline per aortic arch morphology			
	No hypoplastic aortic arch	**Hypoplastic aortic arch**	**P-value[a]**
	(n=51)	**(n=14)**	
Age at initial repair (years)	4.8 (0.1-12.9)	7.3 (2.8-20.3)	0.159
Aortic arch			
Diameter (mm)	22 (19-25)	21 (18-22)	0.193
Wall surface area (cm^2)	41 (33-53)	40 (34-46)	0.768
Volume (cm^3)	19 (10-29)	15 (12-18)	0.604
Hypertension	31 (61%)	13 (93%)	0.025
Left ventricular mass indexed (g/m^2)	80 (70-103)	96 (74-112)	0.411
Residual stenosis (%)	13 (0-28)	16 (13-29)	0.403
Aortic tortuosity	2.2 (1.9-2.6)	2.6 (2.2-3.0)	0.030
Mean torsion aortic arch (dm^{-1})	15 (11-21)	17 (17-22)	0.153
Mean aortic arch curvature (dm^{-1})	4.4 (3.9-5.2)	3.7 (3.0-4.4)	0.027
Median with interquartile range, or number with percentage. [a] Hypoplastic vs no hypoplastic aortic arch.			

Supplemental table 6 intra-observer agreement (n=15)			
	Bland-Altman		**ICC (95% CI)**
	Diff	**LoA**	
Ascending aorta			
Diameter (mm)	0.20	3.34	0.932 (0.812-0.977)
Wall surface area (cm^2)	0.99	18.68	0.953 (0.867-0.984)
Volume (cm^3)	2.41	19.38	0.951 (0.864-0.983)
Ratio ascending descending diameter	-0.01	0.12	0.959 (0.849-0.989)
Aortic arch			
Diameter (mm)	0.29	2.82	0.959 (0.886-0.986)
Wall surface area (cm^2)	1.06	9.85	0.942 (0.841-0.980)
Volume (cm^3)	2.62	15.76	0.789 (0.493-0.923)
Descending aorta			
Diameter (mm)*	-0.01	2.61	0.928 (0.734-0.982)
Wall surface area (cm^2)*	-0.69	29.70	0.874 (0.568-0.967)
Volume (cm^3)*	-0.78	19.96	0.904 (0.657-0.904)
Residual stenosis (%)*	-2.17	9.83	0.867 (0.549-0.965)
Minimal luminal area descending aorta (mm^2)	20.61	80.28	0.934 (0.800-0.978)
Aortic tortuosity*	-0.01	0.74	0.872 (0.562-0.967)
Mean torsion aortic arch (dm^{-1})	-1.64	12.81	0.530 (0.057-0.812)
Mean aortic arch curvature (dm^{-1})	-0.05	1.07	0.819 (0.541-0.935)
Intraclass correlation coefficient are reported with corresponding 95% confidence intervals; *4D flow-based measurements were excluded from repeatability assessment for measurements concerning the distal part of the descending aorta. CI = confidence interval; Diff = mean difference; ICC = intraclass correlation coefficient; LoA = limits of agreement.			

Supplemental table 7 associations with hypertension

Variable	Univariable analysis		Multivariable analysis	
	OR (95% CI)	p-value	OR (95% CI)	p-value
Male sex	1.33 (1.07-1.66)	0.013	2.75 (1.45-5.21)	0.003
Age at scan (years)*	1.05 (1.01-1.10)	0.025		
Age at repair (years)*	1.11 (1.05-1.17)	<0.001	1.31 (1.08-1.60)	0.006
Bicuspid aortic valve	1.16 (0.89-1.52)	0.267		
End-to-end anastomosis	0.99 (0.77-1.28)	0.937		
Left ventricular mass indexed (g/m^2)†	1.08 (1.01-1.16)	0.020	1.00 (1.00-1.00)	0.637
Type of coarctation	0.91 (0.79-1.04)	0.168	0.90 (0.80-1.01)	0.092
Gothic	0.98 (0.77-1.25)	0.894		
Hypoplastic aortic arch	1.38 (1.05-1.80)	0.023	1.29 (1.00-1.66)	0.051
Residual stenosis (%)	1.00 (1.00-1.01)	0.368		
Minimal luminal area descending aorta (mm^2)	1.00 (1.00-1.00)	0.892		
Aortic tortuosity	0.95 (0.80-1.13)	0.586	0.85 (0.73-0.99)	0.047
Aortic arch torsion (dm^{-1})	1.01 (0.99-1.03)	0.175		
Aortic arch curvature (dm^{-1})	0.93 (0.94-1.04)	0.197	0.95 (0.87-1.05)	0.326
Ratio ascending descending diameter	0.94 (0.82-1.09)	0.433		

Multivariable logistic regression model with LASSO regression for variable selection in multivariable analysis. Estimates are given as OR per one unit increase of the variable. *Per five year increase, †LV mass index per 25 grams/m^2. CI = confidence interval, LASSO = least absolute shrinkage and selection operator.

Supplemental table 8 Associations with cardiovascular events

Variable	Univariable analysis		Multivariable analysis	
	HR (95% CI)	p-value	HR (95% CI)	p-value
Male sex	3.17 (1.06-9.47)	0.039	2.07 (0.67-6.41)	0.206
Weight (kg)	1.01 (0.98-1.03)	0.655		
Height (cm)	1.02 (0.98-1.06)	0.397		
Smoking	2.14 (0.96-4.80)	0.064		
Hypercholesterolemia	2.07 (0.68-6.27)	0.199		
Diabetes mellitus	2.24 (0.51-9.76)	0.285		
Age at scan (years)*	1.34 (1.13-1.59)	<0.001	1.18 (0.96-1.44)	0.112
Age at repair (years)*	1.17 (0.97-1.43)	0.097		
Bicuspid aortic valve	3.30 (0.76-14.25)	0.110		
Aortic valve stenosis (≥ moderate)	2.72 (0.98-7.54)	0.055		
Aortic valve regurgitation (≥ moderate)	3.14 (0.88-11.19)	0.077		
End-to-end anastomosis	1.11 (0.44-2.80)	0.826		
Left ventricular mass indexed (g/m^2)†	1.38 (1.13-1.67)	<0.001	1.38 (1.07-1.78)	0.014
Hypoplasia	0.99 (0.37-2.63)	0.978		
Crenel	2.19 (0.83-5.73)	0.112		
Residual stenosis (%)	1.01 (0.98-1.03)	0.692		
Minimal luminal area descending aorta (mm^2)	1.00 (1.00-1.01)	0.035		
Aortic tortuosity	2.20 (1.18-4.10)	0.013	2.20 (0.94-5.17)	0.070
Aortic arch torsion (dm^{-1})	1.02 (0.95-1.09)	0.608		
Aortic arch curvature (dm^{-1})	1.05 (0.70-1.58)	0.808		
Ratio ascending descending diameter	1.39 (0.76-2.53)	0.286		

Time dependent Cox regression model with LASSO regression for variable selection in multivariable analysis. Estimates are given as yearly hazard ratio per one unit increase of the variable. *Per five year increase, †LV mass index per 25 grams/m^2. CI = confidence interval; HR = hazard ratio; LASSO = least absolute shrinkage and selection operator.

Supplemental references

1. Hiratzka LF, Bakris GL, Beckman JA, Bersin RM, Carr VF, Casey DE, et al. 2010 ACCF/AHA/AATS/ACR/ASA/SCA/SCAI/SIR/STS/SVM guidelines for the diagnosis and management of patients with thoracic aortic disease: Executive summary: A report of the american college of cardiology foundation/american heart association task force on pra. Circulation. 2010;121(13):266–369.

2. Hicks KA, Mahaffey KW, Mehran R, Nissen SE, Wiviott SD, Dunn B, et al. 2017 cardiovascular and stroke endpoint definitions for clinical trials. Circulation. 2018;137(9):961–72.